EMBO reports

scientific report

Crystal structure of CbpF, a bifunctional choline-binding protein and autolysis regulator from *Streptococcus pneumoniae*

Rafael Molina[1], Ana González[2]*, Meike Stelter[3], Inmaculada Pérez-Dorado[1], Richard Kahn[3], María Morales[2], Susana Campuzano[2], Nuria E. Campillo[4], Shahriar Mobashery[5], José L. García[2], Pedro García[2] & Juan A. Hermoso[1+]*

[1]Grupo de Cristalografia Macromolecular y Biologia Estructural, Instituto Química-Física Rocasolano, CSIC, Madrid, Spain, [2]Departamento de Microbiologia Molecular, Centro de Investigaciones Biológicas, CSIC, and Ciber de Enfermedades Respiratorias, Madrid, Spain, [3]Laboratoire de Cristallographie Macromoléculaire, Institut de Biologie Structurale J.-P. Ebel CEA-CNRS-UJF, Grenoble, France, [4]Departamento de Quimioterapia, Instituto de Química Médica, CSIC, Madrid, Spain, and [5]Department of Chemistry and Biochemistry, University of Notre Dame, Notre Dame, Indiana, USA

Phosphorylcholine, a crucial component of the pneumococcal cell wall, is essential in bacterial physiology and in human pathogenesis because it binds to serum components of the immune system and acts as a docking station for the family of surface choline-binding proteins. The three-dimensional structure of choline-binding protein F (CbpF), one of the most abundant proteins in the pneumococcal cell wall, has been solved in complex with choline. CbpF shows a new modular structure composed both of consensus and non-consensus choline-binding repeats, distributed along its length, which markedly alter its shape, charge distribution and binding ability, and organizing the protein into two well-defined modules. The carboxy-terminal module is involved in cell wall binding and the amino-terminal module is crucial for inhibition of the autolytic LytC muramidase, providing a regulatory function for pneumococcal autolysis.

Keywords: CBP family; crystallography; pneumococcus; CbpF; virulence

EMBO reports (2009) **10**, 246–251. doi:10.1038/embor.2008.245

[1]Grupo de Cristalografia Macromolecular y Biologia Estructural, Instituto Química-Física Rocasolano, CSIC, Serrano 119, 28006 Madrid, Spain
[2]Departamento de Microbiologia Molecular, Centro de Investigaciones Biológicas, CSIC, and Ciber de Enfermedades Respiratorias, Ramiro de Maeztu 9, 28040 Madrid, Spain
[3]Laboratoire de Cristallographie Macromoléculaire, Institut de Biologie Structurale J.-P. Ebel CEA-CNRS-UJF, 41 rue Jules Horowitz, 38027 Grenoble Cedex 1, France
[4]Departamento de Quimioterapia, Instituto de Química Médica, CSIC, Juan de la Cierva 3, 28006 Madrid, Spain
[5]Department of Chemistry and Biochemistry, University of Notre Dame, Notre Dame, Indiana 46556, USA
*These authors contributed equally to this work
[+]Corresponding author. Tel: +34 91 5619400; Fax: +34 91 5642431; E-mail: xjuan@iqfr.csic.es

Received 25 June 2008; revised 2 December 2008; accepted 4 December 2008; published online 23 January 2009

INTRODUCTION

The Gram-positive bacterium *Streptococcus pneumoniae* is one of the most important human pathogens, which is commensal to the nasopharyngeal cavity. However, under appropriate conditions, pneumococci are able to cause invasive infections such as sepsis and meningitis (Cartwright, 2002). *S. pneumoniae* is unique among prokaryotes due to an absolute requirement for choline in growth, which is incorporated as phosphorylcholine into the cell wall teichoic acid and the membrane lipoteichoic acid (Tomasz, 1967). Choline is recognized by components of the host innate immune system, such as C-reactive protein and the receptor of the platelet-activating factor (Cundell *et al*, 1995). In addition, choline anchors a special class of pneumococcal proteins, referred to as choline-binding proteins (CBPs), to the cell wall by non-covalent interactions. These proteins are involved in a wide range of physiological functions, particularly adhesion to human cells (PspA, CbpA and CbpG; Bergmann & Hammerschmidt, 2006), as cell wall lytic enzymes (LytA, LytB, LytC and Pce; López & García, 2004), or in competence for genetic transformation (LytA, LytC and CbpD; Claverys & Havarstein, 2007). Many of these surface proteins are virulence factors that contribute to the pathogenesis of this organism. CBPs share a modular organization consisting of a biologically active domain and a conserved choline-binding module (CBM). So far, full-length three-dimensional structures of CBPs are available for the phage-encoded lysozyme Cpl-1 (Hermoso *et al*, 2003) and pneumococcal Pce (Hermoso *et al*, 2005).

Here, we describe, for the first time, the crystal structure of CbpF, a member of a new subfamily of the CBPs that are strictly composed of a combination of canonical and non-conserved choline-binding motifs. CbpF is divided into two differentiated modules with specific mechanistic roles. Biochemical studies show that CbpF modulates the enzymatic activity of pneumococcal

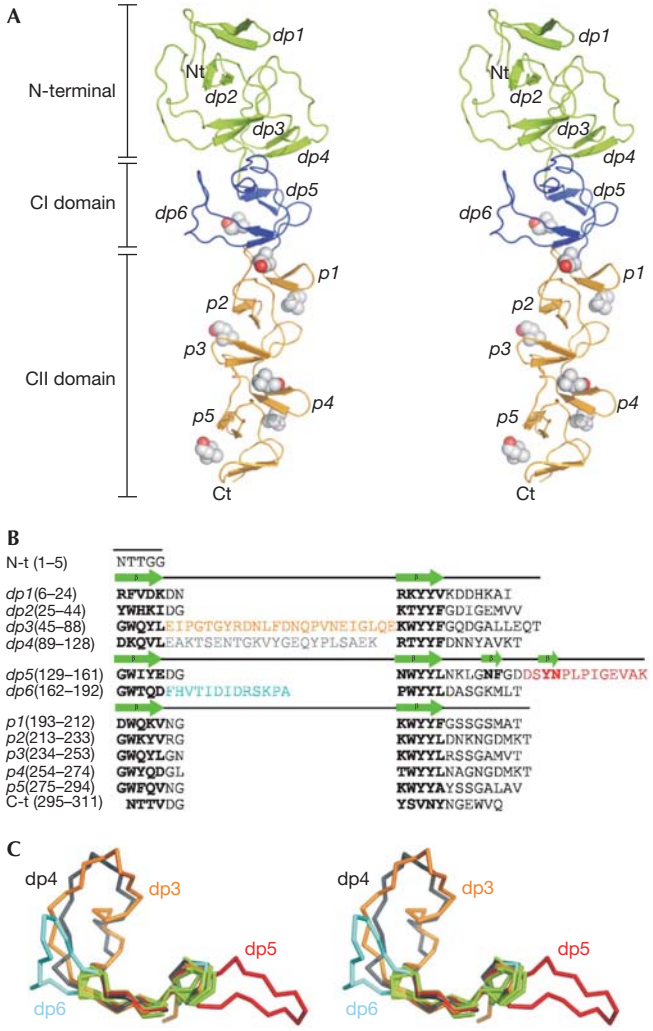

Fig 1 | Three-dimensional structure of CbpF in complex with choline. (**A**) The stereo view of the backbone of CbpF with the amino-terminal module in green, the CI domain in blue and CII domain in orange. Individual choline molecules bound to the choline-binding sites are drawn as space-filled models. (**B**) Complete sequence of CbpF. Comparison of the amino-acid sequence composition of the choline-binding repeats. Canonical repeats are labelled as *p* and modified repeats are *dp*. Amino acids folded in β-strands are shown in bold. (**C**) The stereo view of the Cα superimposition of all choline-binding repeats. Canonical choline-binding repeats *p1–p5* and also modified repeats *dp1* and *dp2* are shown in green, *dp3* in orange, *dp4* in grey, *dp6* in light blue, and *dp5* in red. R.m.s.d. values among *p1–p5* repeats range from 0.30 to 0.70 Å; greater differences are observed between canonical and modified repeats (0.44 to 1.02 Å, as obtained by the superimposition of the *p1* repeat on the *dp1–dp6* repeats). CbpF, choline-binding protein F.

murein hydrolases, suggesting that this CBP could be essential in the regulation of these crucial enzymes.

RESULTS AND DISCUSSION

Overall structure of the CbpF–choline complex

CbpF was crystallized, and its structure was solved by the single-wavelength anomalous diffraction (SAD) technique. CbpF is folded into two well-defined modules (Fig 1). The amino-terminal module (residues 1–128) shows a disc-shape conformation (37 Å × 34 Å × 24 Å). The CBM (residues 129–311) follows the superhelical fold previously found in other CBPs and is arranged into two regions referred to as CI and CII (Fig 1A). The CII domain (residues 193–311) presents five choline-binding repeats (p1–p5) of around 20 amino acids each, with the consensus motif (GWXK-X_{4-5}-WYY-hydrophobic-X_{3-5}-GXMX_{2-3}), and a carboxy-terminal tail of 16 amino acids (295–311). Each repeat comprises a symmetrical β-hairpin, followed by a loop and a coiled region. The CI structural domain of CbpF (residues 129–192) presents two modified choline-binding repeats (dp5 and dp6) showing additional amino acids inside the β-hairpin of the dp6 repeat and also in the loop after the β-hairpin of the dp5 repeat (coloured in red and cyan in Fig 1B). The CI domain defines a linker region between the N-terminal module and the CBM.

The structure of CbpF has unique features compared with other CBPs, as it is assembled entirely by choline-binding repeats. In the CII domain, the repeats strictly follow the consensus motif, whereas in the CI domain they are moderately modified by amino-acid insertions. Notably, the repeats building the N-terminal module are highly modified by both additional amino acids and mutations on different positions of the consensus motif (see Fig 1B). The presence of this choline-binding repeat framework along the sequence produces the elongated shape of CbpF (>117 Å long) and results in a good structural superimposition of both canonical and modified repeats (Fig 1C).

The crystal structure of CbpF in complex with choline shows that up to seven choline-binding sites are available (Fig 1). These seven choline molecules are all located at the CBM in such a way that at least three structurally conserved aromatic residues (two tryptophans from a repeat and one tyrosine from the next repeat) plus one hydrophobic residue (methionine or leucine) form a cavity in which choline methyl groups are placed (Fig 2A). This binding-site framework is observed in both CI and CII domains; however, the N-terminal module does not fulfil the choline-binding requirements. We note that in dp1, dp2 and dp4 repeats at least one of the crucial tryptophan residues is replaced by threonine or lysine (Fig 1B). It would seem that this mutational replacement of residues produces a reduction in choline-binding ability and that, in the case of the lysine residues, the formation of crucial salt bridge interactions affects modular rearrangement (see below).

Sequence divergence in the choline-binding repeats

Sequence divergence observed in CbpF is generated by mutations of the consensus amino-acid residues of the repeat, by amino-acid additions in the β-hairpin turn or the loop, or by a combination of both (Fig 1B). The high divergence of the first four repeats (dp1–dp4) is responsible for the absence of choline-binding capacity at the N-terminal region. Besides, modifications in the nature and composition of the choline-binding repeats crucially alter other features of CbpF. Amino-acid additions observed in dp3, dp4, dp5 and dp6 repeats (Fig 1B) result in longer repeats of 43, 39, 32 and 30 amino acids, respectively, compared with the 20 amino acids of a canonical choline-binding repeat. Variations in the sequence of the choline-binding repeats are also responsible for the modular arrangement in CbpF. Intermodular interactions are carried out through the N-terminal module and the CI domain. Lys 90 is at a

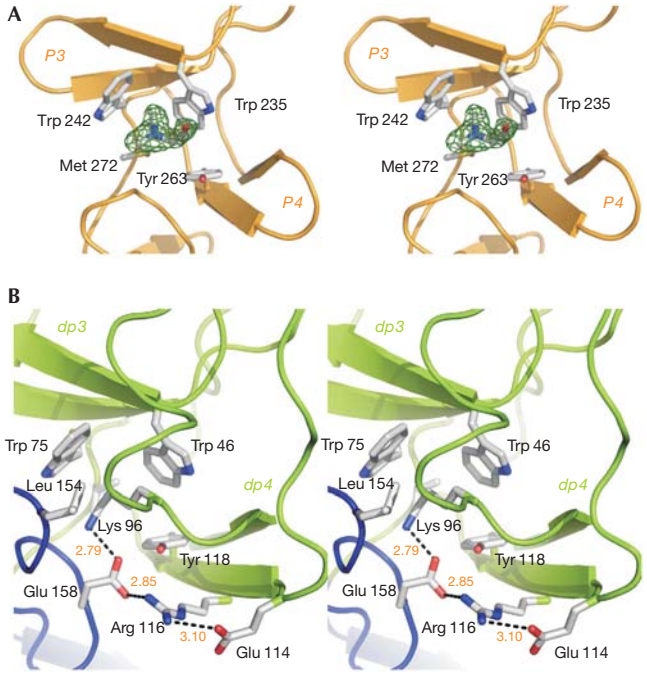

Fig 2 | Choline-binding sites at the carboxy- and amino-terminal modules. (**A**) Stereo view of the choline molecule bound to a canonical choline-binding site, showing its F_o-F_c electron density omit map contoured at 3σ (green). (**B**) At the N-terminal module, only one pocket presents all residues required for choline binding. However, Lys 96 residue is blocking this site and establishing a network of salt bridge interactions crucial in the modular arrangement of CbpF.

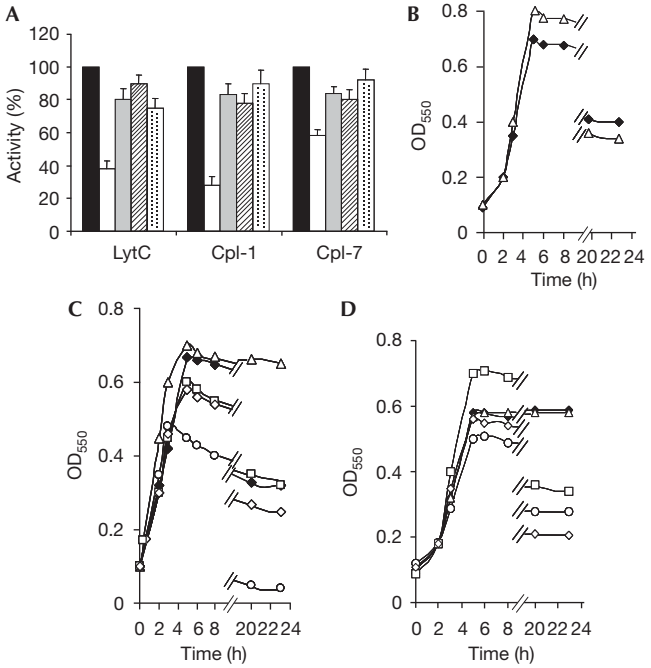

Fig 3 | Inhibitory effect of CbpF on LytC hydrolytic activity. (**A**) *In vitro* cell wall lytic activity of LytC, Cpl-1 and Cpl-7 enzymes without CbpF (black bars), with addition of 0.2 μM CbpF (white bars), 0.2 μM C-LytA (grey bars), 0.2 μM C-CbpF (hatched bars) or 0.2 μM N-CbpF (dotted bars). The error bar is estimated as a triple of the standard deviation ($n = 5$ experiments). (**B**) Growth curves of R6*lytA* (closed diamonds) and R6*lytAcbpF* (open triangles) strains at 30 °C. (**C**) Sensitization of the R6*lytA* strain by externally added, purified proteins, at 1.2 μM final concentration. An exponentially growing culture (OD_{550}=0.2), at 30 °C, of the R6*lytA* strain had CbpF (open triangles), C-CbpF (open circles), C-LytA (open squares), or LytB (open diamonds) added. The growth curve of an untreated culture of R6*lytA* (closed diamonds) is also shown. (**D**) The effect of different proteins on LytC activity assayed in a culture of R6*lytAlytC* strain by externally added purified proteins, at 1.2 μM final concentration. An exponentially growing culture (OD_{550}=0.2), at 30 °C, of the R6*lytAlytC* strain had LytC (open diamonds), LytC + CbpF (open triangles), LytC + C-CbpF (open circles), or LytC + LytB (open squares) added. The growth curve of an untreated culture of R6*lytAlytC* (closed diamonds) is also shown. R6, wild-type strain of *Streptococcus pneumoniae*.

salt bridge interaction distance of Asp 89 (3.37 Å), and Lys 96 connects the N-terminal module and the CBM (Fig 2B).

CbpF modulates the autolytic function of LytC

A highly sensitive and reliable method with radioactive pneumococcal cell wall as a substrate has been implemented to detect lytic activities of the pneumococcal cell wall. By using this assay, CbpF did not show any lytic activity, indicating that it is unlikely that CbpF has such enzymatic activity. Nevertheless, we tested whether CbpF could affect the activity of the known pneumococcal murein hydrolases (LytA, LytB, LytC and Pce). We assumed that CbpF could modulate the cell wall hydrolytic activities of these enzymes either by competing for the choline-binding sites or for their substrate or by interacting with their catalytic or binding modules. To test this hypothesis, we determined the *in vitro* cell wall lytic activity of different murein hydrolases in the presence of CbpF or the isolated homologous CBM of LytA (C-LytA). The results showed that LytA, LytB and Pce activities were not essentially affected by the addition of CbpF, but that the activity of the LytC lysozyme was reduced in the presence of 200 nM CbpF (supplementary Fig S2 online). To investigate the possible individual contribution of the isolated modules of CbpF to this inhibitory effect, N-CbpF- (containing the first 192 amino acids) or C-CbpF- (containing the CII domain; supplementary information online) truncated proteins were used in a similar radioactive *in vitro* experiment. C-CbpF did not alter the enzymatic activity of LytC, suggesting that the N-terminal domain of CbpF might be crucial in this specific inhibition. Nevertheless, the presence of the anchoring module of CbpF is required for its inhibitory function, because the isolated N-CbpF was unable to inhibit the LytC activity (Fig 3A). These observations preclude the possibility that the inhibitory effect of CbpF on LytC could simply be ascribed to a competition for binding of choline residues of the cell surface, but the binding to choline residues is crucial to keep the CbpF protein in close contact with the cell wall. Although the N-CbpF is able to bind to the peptidoglycan (see below), this interaction seems too weak to prevent the access of LytC to the substrate. This result agrees with the behaviour of other CBP murein hydrolases, in

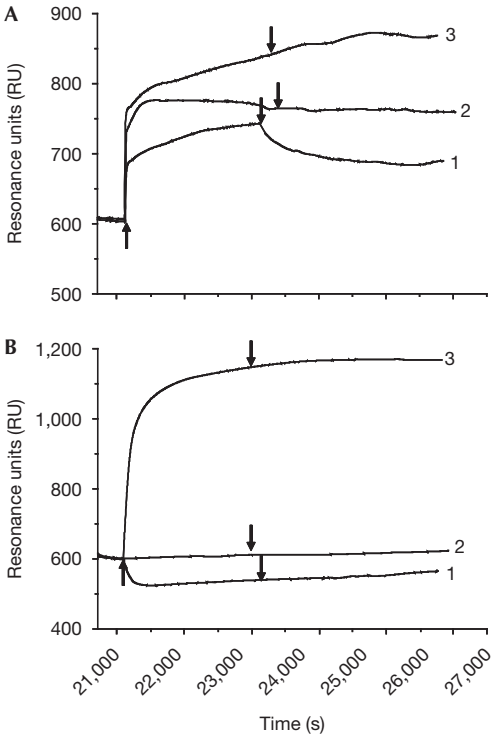

Fig 4 | Analyses of surface plasmon resonance binding. (**A**) Binding curves of CbpF protein to immobilized, purified samples of bacterial cell walls: *Micrococcus lysodeikticus* (1), non-choline *Streptococcus pneumoniae* (2) and choline *S. pneumoniae* (3). (**B**) Binding curves of C-LytA (1), C-CbpF (2) and N-CbpF (3) to non-choline immobilized *S. pneumoniae* cell wall. The leftmost arrow in each graph indicates injection of 2.7 μM protein in 0.1 M Tris–HCl pH 8.0 containing 38.5 mM choline buffer; the three right-hand arrows in each graph indicate injection of the same buffer without protein.

which the absence of the CBM reduces their functional activity to practically undetectable levels (Sanz *et al*, 1992).

To test whether the inhibitory effect of CbpF could affect other pneumococcal lysozymes and to confirm that this effect was not due to a binding competition for choline residues of cell wall, we assayed the pneumococcal phage lysozymes Cpl-1 and Cpl-7. Despite only the three-dimensional structure of Cpl-1 having been reported, sequence and biochemical analyses show that although the catalytic modules of both phage lysozymes are similar, the anchoring modules are completely different (Cpl-7 does not bind to choline; García *et al*, 1990). Notably, both enzymes were inhibited by CbpF (Fig 3A), suggesting that the inhibitory effect is not limited to the LytC lysozyme and that the effect is not due to competition for choline residues.

As the LytC lysozyme is involved in the autolysis of pneumococcal cultures at 30 °C (García *et al*, 1999), we used this property to investigate the role of CbpF *in vivo*. Therefore, we analysed the effect on autolysis of the absence or exogenous addition of CbpF in R6*lytAcbpF*, a double frameshift/insertion mutant of the wild-type R6 *S. pneumoniae* strain. The mutant was LytA-deficient to avoid the effect of this principal autolysin on the autolytic role of LytC at 30 °C. The slow autolysis curve for R6*lytA* (López *et al*, 1986), a single frameshift mutant of R6, at 30 °C was accelerated in the R6*lytAcbpF* strain (Fig 3B), suggesting that the absence of CbpF facilitates the autolytic process by LytC. This result agrees with the repression effect of LytC by CbpF observed *in vitro*, indicating that CbpF has the same regulatory function *in vivo*. Furthermore, when we analysed the growth of the R6*lytA* strain in the presence of CbpF added to the bacterial growth (i.e. the surface), we observed that the addition of 1.2 μM CbpF abolished LytC-induced autolysis at 30 °C, whereas the addition of the truncated proteins C-CbpF or C-LytA did not alter the autolytic curve (Fig 3C). The culture containing exogenous CbpF showed the presence of typical unlysed R6*lytA* cells with a short-chain cell morphology under phase-contrast microscopy, whereas many lysed cells were observed in the culture without CbpF, indicating that CbpF protects the cell wall from lytic damage (data not shown).

Conversely, we tested the behaviour of R6*lytAlytC*, a double frameshift/insertion mutant, in the presence of LytC alone or LytC plus CbpF (Fig 3D). As expected, the mutant cells autolysed when they received a defined quantity of LytC (García *et al*, 1999); however, the autolysis was circumvented when LytC was added in the presence of 1.2 μM of CbpF. It is worth noting that the inhibition of this autolytic process did not take place in the presence of similar amounts of C-CbpF or other homologous proteins such as LytB.

Taken together, all these results argue that CbpF selectively modulates the autolytic function of the LytC lysozyme and that the divergent choline-binding repeats that build its N-terminal domain have a crucial function in this effect. It is well established that autolysins have various fundamental roles in bacterial physiology and pathology (Gosink *et al*, 2000; López *et al*, 2004). These catalytically competent enzymes are able to hydrolytically change the integrity of the cell wall of the bacterium itself. The effect of uncontrolled reactions catalysed by these enzymes could be detrimental, and as such the enzymic activity must be tightly regulated. The nature of this regulatory process remains unknown, although there might be some contribution by the lipoteichoic acid in the cell membrane (Höltje & Tomasz, 1975). Recently, the involvement of small non-coding RNAs in the control of stationary-phase autolysis has also been suggested (Halfmann *et al*, 2007). Our results show that CbpF can inhibit the activity of LytC both *in vitro* and *in vivo* and, therefore, we assert that CbpF is crucial in the regulation of the activity of LytC.

The N-terminal module and peptidoglycan interaction

Initial experiments to investigate a possible direct LytC–CbpF interaction, carried out by surface plasmon resonance and crosslinking tests, were negative. Therefore, the observed inhibition caused by CbpF on pneumococcal lysozymes could be due to specific interactions between CbpF and peptidoglycan, preventing access of the lysozyme to its substrate. To study this hypothesis, we analysed these interactions by using surface plasmon resonance—immobilizing cell walls from *Micrococcus lysodeikticus* and from *S. pneumoniae* with and without choline. As expected, CbpF was able to bind tightly to the pneumococcal choline-containing cell wall. Interestingly, CbpF was also able to bind to the cell wall from *S. pneumoniae* without choline and, to a

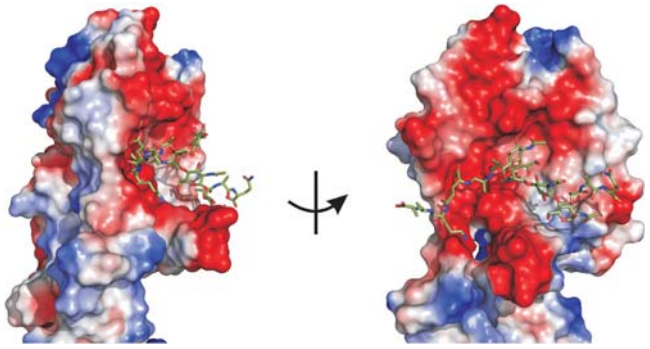

Fig 5 | Model of peptidoglycan docked in the amino-terminal module of CbpF. Electrostatic potential is represented on the molecular surface of CbpF. The synthetic peptidoglycan moiety $(2S5P)_2$ interacting with the N-terminal module is represented as capped sticks.

lesser extent, the cell wall of *M. lysodeikticus*, a standard Gram-positive bacterial peptidoglycan that does not contain choline (Fig 4A). Furthermore, truncated C-CbpF and C-LytA proteins were not able to bind to the pneumococcal cell wall without choline, suggesting that their binding capacity is restricted to their specific interaction with this amino-alcohol (Fig 4B). Notably, the isolated N-CbpF was able to bind to the pneumococcal cell wall without choline, suggesting that N-CbpF is able to specifically recognize the pneumococcal cell wall and that the N- and C-terminal modules of CbpF bind to different components of the peptidoglycan.

The N-terminal module of CbpF shows a markedly different three-dimensional structure from the CBM. Electrostatic potential on the surface is also different in the two modules.

Docking analyses have shown that pneumococcal peptidoglycan can be accommodated perfectly at the N-terminal cavity of CbpF (Fig 5), reinforcing the hypothesis that CbpF might act by blocking the access of LytC to its substrate. A fragment of the peptidoglycan ([GlcNAc-MurNAc-(L-Ala-γD-Glu-L-Lys-D-Ala-D-Ala)]$_2$) $(2S5P)_2$ interacts with aromatic and hydrophobic residues of the cleft (Tyr 35, Tyr 48, Trp 75, Pro 153 and Leu 154) and with polar residues (Asp 38, Glu 50 and Asn 152; supplementary Table S2 online). Crystallization trials failed to provide direct information on peptidoglycan binding at the CbpF N-terminal module. Native crystals fractured when put in contact with the synthetic cell wall fragment, and only in one case with a rapid soak could a diffraction data set be collected (supplementary Table S1 online). Despite the absence of electron density for peptidoglycan, the presence of the ligand caused a significant alteration of the CbpF structure at the CI domain and at the N-terminal module (supplementary Fig S1 online). Long loops of the CI domain of the complexed structure are highly disordered and it was not possible to trace even the backbone between residues 168 and 178. The N-terminal module in the presence of the peptidoglycan analogue rotated ~10° around a molecular hinge between the N-terminal module and the linker region, leading to large differences in the relative positions between the modules, and further supporting a direct interaction between the peptidoglycan and the N-terminal module.

CbpF heads a protein family of unknown function

A study of the CbpF orthologues in other pneumococcal strains has showed the existence of proteins CbpC and CbpJ in the TIGR4 strain (supplementary Figs S3 and S4 online). Notably, a comparative analysis of the genes that encode these proteins shows that *cbpF* might have resulted from the recombination of *cbpC* and *cbpJ*. The coexistence of two highly similar genes in the TIGR4 strain indicates that the corresponding encoded CbpF-like proteins have a crucial physiological function and that this duplication might favour the acquisition of more selective regulatory properties.

Further analyses of known pneumococcal genomes show the existence of several proteins that are likely to show the same architecture as CbpF. These proteins might constitute a new CbpF-like subfamily, within the large CBP family of proteins, that have a typical CBM and an N-terminal region formed by a series of non-consensus repeats. Despite the minor differences in amino-acid composition among all the members of the CbpF-like subfamily, most of the residues involved in both the N-terminal structural framework and in the intermodular interactions are preserved, indicating that these proteins might have similar regulatory functions to CbpF.

Concluding remarks

We have disclosed the structure and fold for CbpF, which is unique among the other functional domains of CBPs so far determined. This structure and the new bifunctional regulatory role that we have documented for CbpF open future avenues of research into the characterization of other pneumococcal members of this new subfamily of CBPs, the structure and function of which remain unknown.

METHODS

Purification, crystallization and *in vitro* assays. CbpF was produced, purified and crystallized as described earlier (Molina *et al*, 2007). Detailed information about *in vitro* assays is described in the supplementary information online.

Structure determination. A gadolinium derivative and a data set at the peak of the Gd LIII absorption edge were obtained. SAD data were collected from frozen crystals at 100 K using a charged couple detector on beamline ID29 at the European Synchrotron Radiation Facility (ESRF). Data processing and structure determination is described in the supplementary information online.

Docking studies. The docking studies were carried out with the FlexiDock module of the SYBYL 6.9 suite of programs (Tripos Inc., St Louis, MO, USA). Detailed information about docking protocols is described in the supplementary information online.

Coordinates. The structure of CbpF–choline and CbpF–$(2S5P)_2$ complexes have been deposited in the Protein Data Bank (accession codes 2v04 and 2vyu).

Supplementary information is available at *EMBO reports* online (http://www.emboreports.org).

ACKNOWLEDGEMENTS

We thank E. García for a critical reading of the paper. This study was supported by grants from the Spanish Ministry of Science and Technology (BFU2005-01645 and SAF2006-00390) and by the COMBACT program of the Comunidad de Madrid (S-BIO-0260/2006) and CIBER de Enfermedades Respiratorias (CIBERES), which is an initiative of Spanish Instituto de Salud Carlos III. R.M. and A.G. hold a fellowship from the

Spanish Ministry of Science and Technology. S.C. holds a Juan de la Cierva fellowship from the Spanish Ministry of Science and Technology. The study in the USA was supported by the National Institutes of Health.

CONFLICT OF INTEREST

The authors declare that they have no conflict of interest.

REFERENCES

Bergmann S, Hammerschmidt S (2006) Versatility of pneumococcal surface proteins. *Microbiology* **152:** 295–303

Cartwright KA (2002) Epidemiology of meningococcal disease. *Hosp Med* **63:** 264–267

Claverys JP, Havarstein LS (2007) Cannibalism and fratricide: mechanisms and raisons d'être. *Nat Rev Microbiol* **5:** 219–229

Cundell DR, Gerard NP, Gerard C, Idanpaan-Heikkila I, Tuomanen EI (1995) *Streptococcus pneumoniae* anchors to activated human cells by the receptor for platelet-activating factor. *Nature* **377:** 435–438

García P, García JL, García E, Sánchez-Puelles JM, López R (1990) Modular organization of the lytic enzymes of *Streptococcus pneumoniae* and its bacteriophages. *Gene* **86:** 81–88

García P, González MP, García E, García JL, López R (1999) The molecular characterization of the first autolytic lysozyme of *Streptococcus pneumoniae* reveals evolutionary mobile domains. *Mol Microbiol* **33:** 128–138

Gosink KK, Mann ER, Guglielmo C, Tuomanen EI, Masure HR (2000) Role of novel choline binding proteins in virulence of *Streptococcus pneumoniae*. *Infect Immun* **68:** 5690–5695

Halfmann A, Kovács M, Hakenbeck R, Brückner R (2007) Identification of the genes directly controlled by the response regulator CiaR in *Streptococcus pneumoniae*: five out of 15 promoters drive expression of small non-coding RNAs. *Mol Microbiol* **66:** 110–126

Hermoso JA, Monterroso B, Albert A, Galán B, Ahrazem O, García P, Martínez-Ripoll M, García JL, Menéndez M (2003) Structural basis for selective recognition of pneumococcal cell wall by modular endolysin from phage Cp-1. *Structure* **11:** 1239–1249

Hermoso JA, Lagartera L, González A, Stelter M, García P, Martínez-Ripoll M, García JL, Menéndez M (2005) Insights into pneumococcal pathogenesis from the crystal structure of the modular teichoic acid phosphorylcholine esterase Pce. *Nat Struct Mol Biol* **12:** 533–538

Höltje JV, Tomasz A (1975) Lipoteichoic acid: a specific inhibitor of autolysin activity in pneumococcus. *Proc Natl Acad Sci USA* **72:** 1690–1694

López R, García E (2004) Recent trends on the molecular biology of pneumococcal capsules, lytic enzymes, and bacteriophage. *FEMS Microbiol Rev* **28:** 553–580

López R, Sánchez-Puelles JM, García E, García JL, Ronda C, García P (1986) Isolation, characterization and physiological properties of an autolytic-deficient mutant of *Streptococcus pneumoniae*. *Mol Gen Genet* **204:** 237–242

López R, García E, García P, García JL (2004) Cell wall hydrolases. In *The Pneumococcus*, Tuomanen EI, Mitchell TJ, Morrison DA, Spratt BG (eds) 75–88. Washington, DC: ASM Press

Molina R, González A, Moscoso M, García P, Stelter M, Kahn R, Hermoso JA (2007) Crystallization and preliminary X-ray diffraction studies of the choline binding protein F from *Streptococcus pneumoniae*. *Acta Crystallogr Sect F Struct Biol Cryst Commun* **63:** 742–745

Sanz JM, Díaz E, García JL (1992) Studies on the structure and function of the N-terminal domain of the pneumococcal murein hydrolases. *Mol Microbiol* **6:** 921–931

Tomasz A (1967) Choline in the cell wall of a bacterium: novel type of polymer-linked choline in *Pneumococcus*. *Science* **157:** 694–697